Dissociation of Oxygen in a Radiofrequency Electrical Discharge

An experimental investigation was made of oxygen dissociation in a radiofrequency discharge. The conversion and yield were examined as a function of power, pressure, and gas flow rate. These measurements were supplemented by measurements taken with catalytic and noncatalytic thermocouple probes in order to determine the local gas temperature and atomic oxygen concentration. An interpretation of the results is given in terms of a theoretical model of the reactor.

ALEXIS T. BELL and KAM KWONG

Department of Chemical Engineering
University of California
Berkeley, California 94720

SCOPE

An interest in the dissociation of oxygen by high frequency electric discharges has been stimulated by the use of atomic oxygen for the formation of thin films of metal oxides (Ligenza, 1965; Secrist and Mackenzie, 1967; O'Hanlon, 1970) and for the removal of polymer films used in the photoengraving of integrated circuits (Irving, 1968). Previous studies of oxygen dissociation (McCarthy, 1954; Francis, 1969; Mearns and Morris, 1971) have been carried out with microwave discharges. These efforts have identified the effects of the experimental variables but have not provided a comprehensive model of the discharge as a reactor.

The purpose of the present study was to investigate the dissociation of oxygen in a radiofrequency discharge and to develop a model for the interpretation of the experimental results. The reactor used in this research had the shape of a pillbox. Two external electrodes placed against the flat ends of the pillbox were used to couple the reactor to a 13.56 MHz generator which supplied the power for the discharge. Gas phase titration with NO_2 was used to detect the presence of atomic oxygen. Measurements of the conversion and yield were made as a function of power, pressure, and flow rate. Additional information was obtained from measurements of the gas temperature and the distribution of atomic oxygen within the reactor with a pair of thermocouple probes.

CONCLUSIONS AND SIGNIFICANCE

Measurements of the overall extent of oxygen dissociation were performed over the following range of conditions: power, 0 to 140 watts; pressure, 2 to 4 torr; and flow rate, 2 to 10 $\times$ 10^{-4} moles/min. Within this range the highest conversions were obtained at high power, low pressure, and low flow rate. The response of the yield to variations in the experimental variables was different, the best yields being obtained at intermediate powers and low pressures. Flow rate had very little effect on the yield.

The gas temperature in a stagnant discharge was found to rise rapidly with power up to a level of 300°C. Increases in pressure produced a slight increase in temperature as did increases in flow rate. The latter effect was attributed to the gas composition which at high flow rates contains more molecular oxygen and hence has a lower thermal conductivity.

The local concentration of atomic oxygen in a stagnant discharge was determined by the temperature difference existing between a catalytic and noncatalytic thermocouple probe. At a fixed point in the reactor the atom concentration was observed to pass through a maximum as either the power or the pressure was varied. Increasing the gas flow rate caused the atom concentration to decrease. Measurements of the radial distribution of atomic oxygen within the reactor showed it to be quite uniform except in the immediate vicinity of the walls.

Visual observations of the discharge showed that the glow tended to be nonuniform, separating into two bright discs located beneath the electrodes. This tendency increased with both power and pressure. A partial explanation for this behavior was derived from an analysis of the spatial distribution of the electric field strength.

A theoretical model of the dissociation kinetics was developed based on a simplified view of the discharge and the assumption of plug flow behavior. Using this model it was possible to predict the conversion and yield as functions of power, pressure, flow rate, and discharge size. These results correctly demonstrated most of the qualitative features of the experimental data. A quantitative comparison with the data could not be achieved since it was concluded that only a fraction of the reactor volume was effective. By forcing a fit between the data and the predictions of the model for a fixed set of conditions it

was found that only 9.4% of the total reactor volume was effective. Further examination showed that the effective volume decreased with flow rate, a pattern which was consistent with the nature of the flow in the reactor.

The major significance of the present work is that it provides a variety of experimental observations of the dissociation of oxygen in a radiofrequency discharge and offers an explanation for these observations in terms of a simple theoretical model. Whereas the model cannot be used to characterize the experimental results quantitatively, it does provide the proper framework for interrelating the physical and chemical phenomena.

High frequency electric discharges offer a convenient and effective means for producing atomic oxygen. Over the past several years an interest in this process has arisen because of the demonstrated use of atomic oxygen in the preparation of thin films of metal oxides (Ligenza, 1965; Secrist and Mackenzie, 1969; O'Hanlon, 1970) and the removal of photo-resist film, a polymer used for the photoengraving of integrated circuits (Irving, 1968). Previous studies of oxygen dissociation have been carried out using microwave discharges. The earliest of these efforts, performed by McCarthy (1954), showed that the yield of atomic oxygen per unit energy could be correlated empirically with the electric field strength, the contact time, the gas pressure, and the shunt impedance of the discharge. In a later effort, Francis (1969) demonstrated that for a fixed power the yield of atomic oxygen passed through a maximum at about 6 torr. From his study of the decay of atomic oxygen outside the discharge he concluded that the principal homogeneous recombination process proceeded through the formation of ozone. Most recently, Mearns and Morris (1971) described extensively the effects of the experimental variables on the conversion and yield of atomic oxygen. The principal factors found to influence the results were (a) the discharge power; (b) the gas pressure; (c) the residence time in the discharge; (d) the surface condition of the discharge tube; and (e) the moisture content of the inlet oxygen.

The purpose of the present study was to investigate the dissociation of oxygen in a radiofrequency discharge and to relate the observed conversions and yields to the experimental conditions. For this purpose measurements were made of the conversion and yield as a function of power, pressure, and flow rate in a reactor of well-defined geometry. Additional information was obtained from measurements of the gas temperature and the distribution of atomic oxygen within the reactor. A model of the reactor was developed in order to assist in the interpretation of the experimental results.

EXPERIMENTAL APPARATUS

The experimental apparatus shown in Figure 1 consisted of the reactor, a gas supply manifold, a power supply, and provisions for detecting atomic oxygen. The reactor, shown in detail in Figure 2, was constructed of Pyrex in the form of a pillbox 8 cm in diameter by 2.5 cm high. Molecular oxygen was supplied to the reactor by a 12 mm O.D. tube and the discharged gas was removed by a similar tube placed diametrically opposite the inlet. Two additional tubes were attached to the reactor at positions perpendicular to the flow. These tubes contained movable thermocouples used to measure temperature profiles across the diameter of the reactor.

Power for the discharge was supplied by an IPC Model 3001 radiofrequency generator operating at 13.56 MHz and capable of delivering up to 150 watts. The generator was connected to a matching network which was in turn connected to silver electrodes painted on the external surface of the flat ends of the reactor. The forward power delivered by the generator as well as that reflected from the load were measured by a watt meter supplied with the generator.

The atomic oxygen produced in the discharge was detected by titration with NO_2. This technique has been reviewed by Kaufman (1961) and more recently by Mearns and Morris (1970). In the present experiments NO_2 was supplied by bubbling a metered stream of helium through a tank of liquid N_2O_4 maintained at 0°C (see Figure 1). Saturation of the helium stream was guaranteed by passing the gas stream through a glass saturator in which a large surface area of liquid N_2O_4 was exposed to the gas. After saturation the flow rate of the gas stream was measured again using a capillary flowmeter and the gas was then expanded into the vacuum system through a Whitey fine metering valve.

To perform a titration the He-NO_2 mixture was mixed with the discharged oxygen 5 cm downstream from the reactor. As the flow rate of the titrating mixture was increased a greenish-yellow glow was produced by the reaction sequence

$$O + NO_2 \rightarrow NO + O_2$$

$$O + NO \rightarrow NO_2 + h\nu$$

The presence of the glow was observed by the naked eye in a darkened room. When the flow rate of NO_2 became equal to that of atomic oxygen the glow was extinguished since no

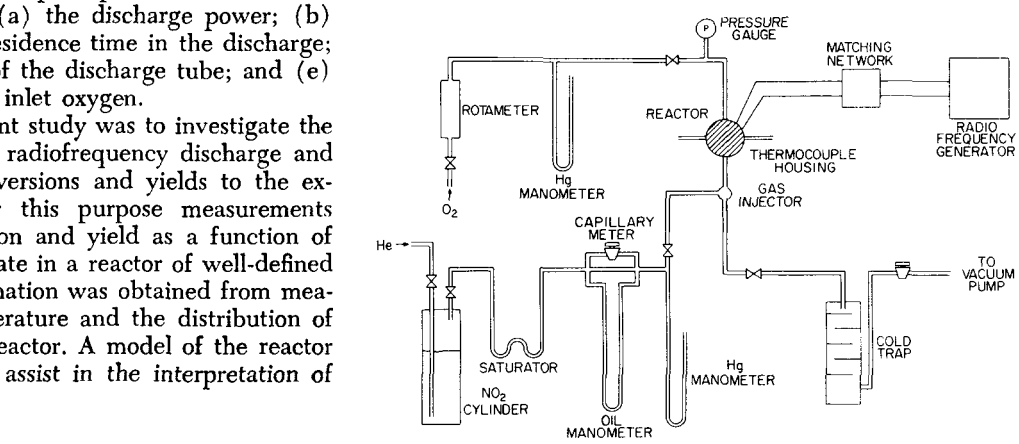

Fig. 1. Schematic of the experimental apparatus

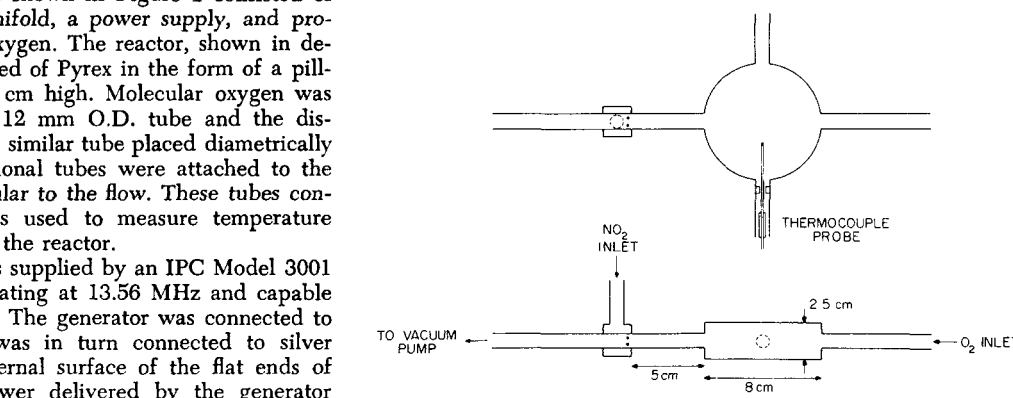

Fig. 2. Schematic of the reactor.

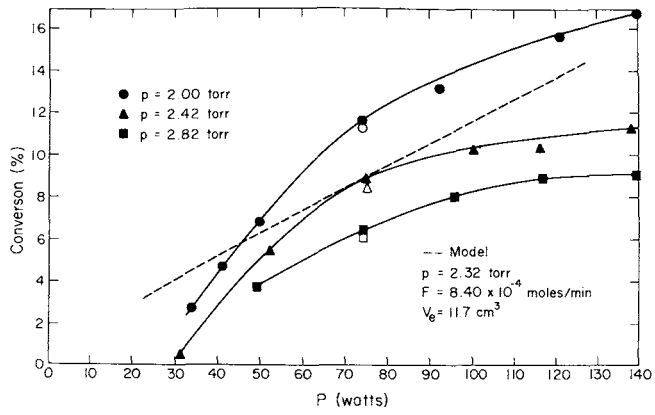

Fig. 3a. Conversion versus power.

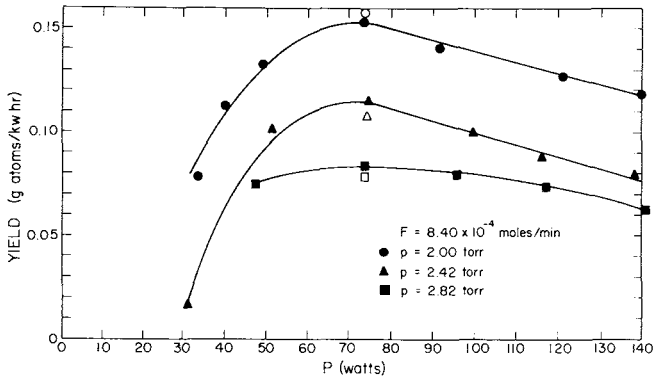

Fig. 3b. Yield versus power.

excess of atomic oxygen remained at this point to react with the NO. Visual observation of the endpoint proved to be satisfactory and provided reproducible results. The flow rate of atomic oxygen measured at the titrating point was taken to be identical to that at the exit from the reactor. An estimate of the fractional loss of atomic oxygen by wall recombination between the reactor and the titrating point showed it to be a maximum of 4% at the lowest flow rate used in these experiments.

Measurements of the gas temperature and the radial distribution of atomic oxygen were made with the aid of small thermocouples inserted through the wall of the reactor. Each of the probes was made by placing a copper-constantan junction made of 32 gauge wire inside a length of Pyrex capillary tubing. The tubing near the junction was then heated to the softening point and pulled carefully so that the junction was buried inside a round globule of glass 2.5 mm in diameter. By this means the thermocouple wires were protected from direct contact with the plasma. A short length of steel tubing was fastened to the outside of the capillary tubing and served to position the probe in the glass tube attached to the reactor. By this means it was possible to move the probe with the aid of an external magnet.

Two identical probes were constructed. The tip of one probe was left bare. Since atomic oxygen recombination on glass is relatively poor ($\gamma \simeq 10^{-4}$) this probe was used to measure the gas temperature. The tip of the second probe was covered with a thin layer of silver paint. Upon exposure to the plasma the organic binder in the paint was removed and the solid material was converted into a black silver oxide. The silver oxide thus formed is known to be a catalyst for oxygen recombination (Elias et al., 1959). To test for the possibility that the coated probe might be responsive to the presence of metastable as well as atomic species, coated and uncoated probes were inserted into a helium discharge which produces metastables alone. This experiment showed no significant difference in the temperatures measured by the two probes. As a result, it was concluded that the difference in temperatures measured in the oxygen discharge was due primarily to the recombination of atomic oxygen and could be used as a measure of the local atomic oxygen concentration.

EXPERIMENTAL RESULTS

The extent of dissociation as well as the yield of atomic oxygen per kilowatt hour of energy were measured as functions of power, pressure, and gas flow rate. These results are shown in Figures 3a, 3b, 4, 5a, and 5b.

For a fixed pressure and flow rate an increase in the discharge power causes the extent of dissociation to increase. This rise is at first rapid but becomes more gradual at higher powers. The yield on the other hand rises to a maximum value at about 75 watts and then decreases at higher powers. It should be noted that the shaded and unshaded symbols used in Figures 3a and 3b and subsequent figures represent data points collected one week

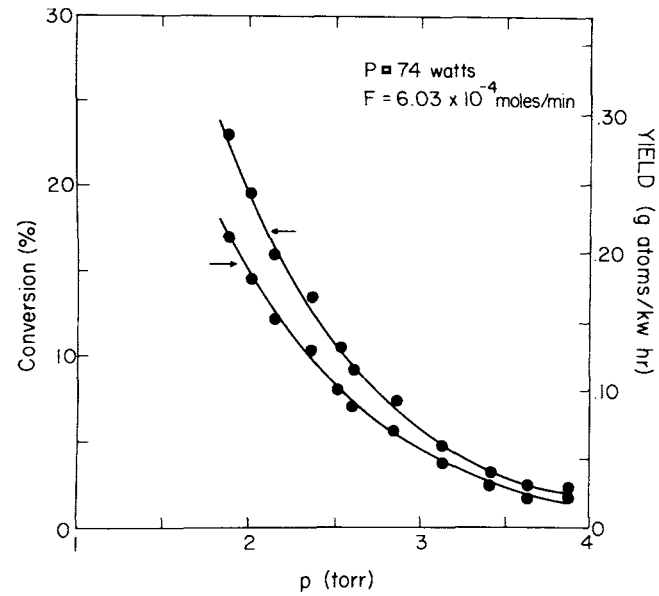

Fig. 4. Conversion and yield versus pressure.

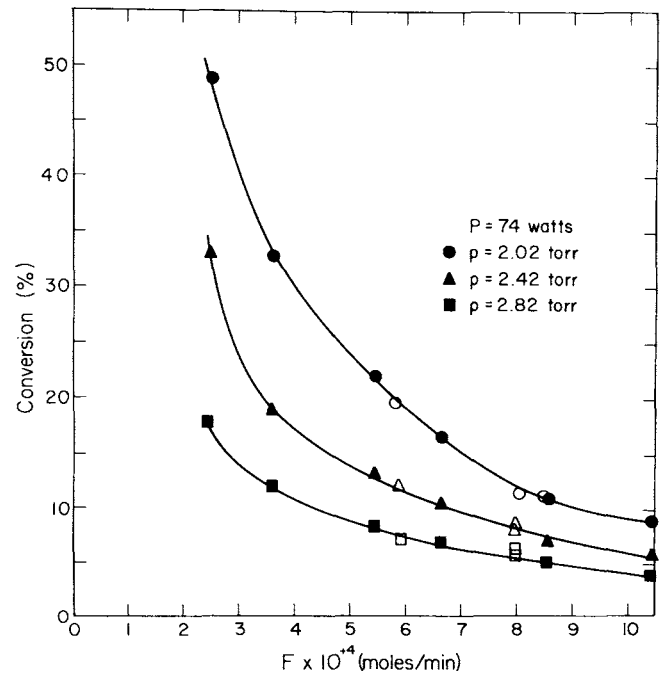

Fig. 5a. Conversion versus flow rate.

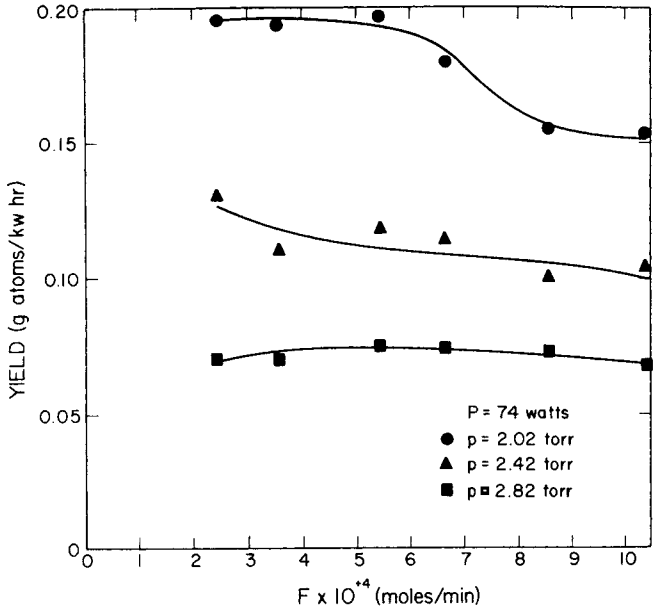

Fig. 5b. Yield versus flow rate.

apart. The close correspondence of the points for a given set of conditions indicates the reproducibility of the data.

The effect of pressure on both the extent of dissociation and yield were studied by maintaining the flow rate and power constant. On this basis the residence time increases with the pressure. The observed decreases in extent of dissociation and yield shown in Figure 4 are, however, due to the increase in gas density occurring with increased pressure.

The effect of oxygen molar flow rate on the extent of dissociation and the yield of atomic oxygen were investigated at 74 watts for pressures of 2.02, 2.42, and 2.82 torr. As each of the curves in Figure 5a shows, the extent of dissociation at first decreases rapidly and then slowly levels off. This effect is more pronounced at the lower pressures where the extent of dissociation is highest. Over the same range of flows the yield was found to be relatively insensitive to the flow rate (Figure 5b).

Temperature measurements were made using both the catalytic and noncatalytic thermocouple probes in order to determine the gas temperature and the relative concentrations of atomic oxygen. Measurements of the effects of power and pressure were done in a stagnant system with both probe tips placed at a radius of 1.5 cm. Figure 6 illustrates the variation of the gas temperature T_g and the temperature difference between the two probes ΔT with power. The gas temperature is seen to increase continuously as the power is raised. In contrast the curve of ΔT passes through a maximum at 35 watts. The shape of the ΔT curve was reproduced at both higher and lower pressures and it was observed that the maximum value of ΔT occurred at higher powers the higher the pressure.

Figures 7a and 7b illustrate the effect of increasing pressure on T_g and ΔT. From the curves in Figure 7a it can be seen that the gas temperature experiences a rapid increase initially but then increases more slowly at higher pressures. For each power level the corresponding curve of ΔT versus pressure (Figure 7b) displays a maximum. The pressure at which the maximum occurs depends on the power and is shifted to higher pressures as the power is increased. A second observation that can be made is that the values of ΔT increase with increasing power for pressures above the maximum in ΔT. At pressures below the maximum the inverse pattern is observed.

The influence of flow rate on the spatial distribution of the gas temperature and the oxygen concentration were investigated both in the presence and absence of flow. These results are shown in Figure 8. From Figure 8 it can be seen that for a given flow rate the gas temperature is a maximum at the center of the discharge and decreases towards the walls. With the exception of the data for 4.7×10^{-4} moles/min., the temperature profiles are parallel to each other. One can also observe that as the flow rate is increased the measured gas temperature rises. This phenomenon is not immediately explainable and will be discussed later.

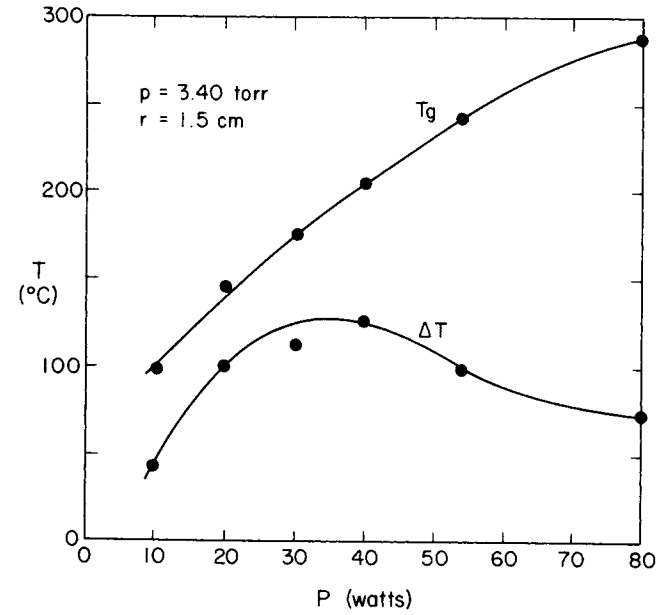

Fig. 6. T_g and ΔT versus power.

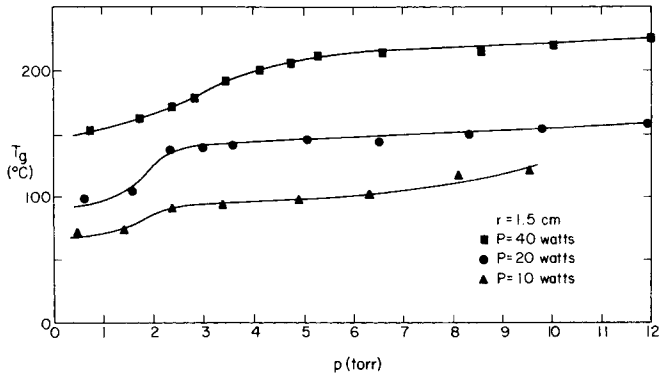

Fig. 7a. T_g versus pressure.

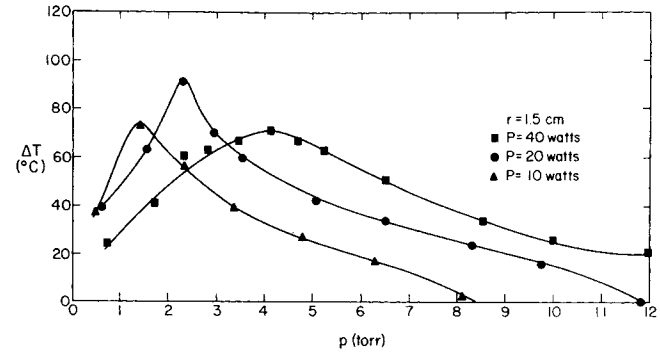

Fig. 7b. ΔT versus pressure.

The curves of ΔT shown in Figure 8 have a fairly flat profile until very near the wall of the reactor which is at 4 cm. Increasing the flow rate causes a decrease in ΔT, indicating a decrease in the concentration of atomic oxygen. This pattern is consistent with the titration data shown in Figure 5a.

In the course of the present experiments it was observed that the glow did not uniformly fill the reactor volume. At higher pressures and power levels a segregation occurred yielding bright glowing areas in the immediate vicinity of the electrodes. Photographs of the reactor were taken to record this effect. Figure 9 shows the change in intensity and distribution of the glow as the power is increased from 30 to 90 watts at a pressure of 3.6 torr. At all power levels it can be seen that the glow concentrates near the electrodes and increases in intensity with power. Figure 9 also illustrates the effects of increasing pressure for a constant power of 20 watts. Here it can be seen that the glow which initially fills the reactor volume breaks into two zones as the pressure is raised. The intensity of the glow is also seen to decrease with increasing pressure.

DISCUSSION

Development of a Reactor Model

A model of the discharge as a reactor was developed in order to relate the experimental variables to the extent of conversion in a rational manner. For this purpose it was assumed that the discharge occurred between two parallel plate electrodes separated from the plasma by a dielectric wall. The electric field strength in the gap was assumed to be constant and the electron density distribution was taken as a cosine distribution. Both of these assumptions are idealizations of the actual behavior (Bell, 1970) but have been made in order to provide a more tractable problem.

The modeling procedure can now be divided into three stages. First is an identification of the mechanism by which atomic oxygen is formed and lost and an evaluation of the rate constants for these primary reactions. Second is a derivation of an expression for the net rate of atomic oxygen production. Third is an estimation of the electron density and average energy as a function of the chosen operating conditions. The last stage is required in order to determine the rate of oxygen dissociation.

The dissociation of molecular oxygen occurs as a result of excitation from the ground state to either the $^3\Sigma_u^+$ or the $^3\Sigma_u^-$ excited state by electron collision. These reactions can be expressed as

$$(1a)\quad e + O_2 \rightarrow O_2^*(A^3\Sigma_u^+) \rightarrow O(^3P) + O(^3P)$$

$$(1b)\quad e + O_2 \rightarrow O_2^*(B^3\Sigma_u^-) \rightarrow O(^3P) + O(^1D)$$

Cross sections for both reactions have been presented by Myers (1969) and are based on the trapped-electron measurements of Schulz and Dowell (1962).

For the present purposes a total dissociation rate constant was determined from the sum of the cross sections for reactions 1a and 1b. The computed rate constant was determined from the expression

$$k_1 = \sqrt{\frac{8}{\pi m_e}}\,(kT_e)^{-3/2}\int_0^\infty \epsilon\sigma_1(\epsilon)e^{-\epsilon/dT_e}\,d\epsilon \quad (1)$$

where σ_1 is the total dissociation cross section. Equation (1) has been derived under the assumption that the electron energy distribution function is Maxwellian. This assumption has been investigated by Myers (1969) and was found to be adequate for excitations whose threshold is not much larger than the average electron energy. Figure

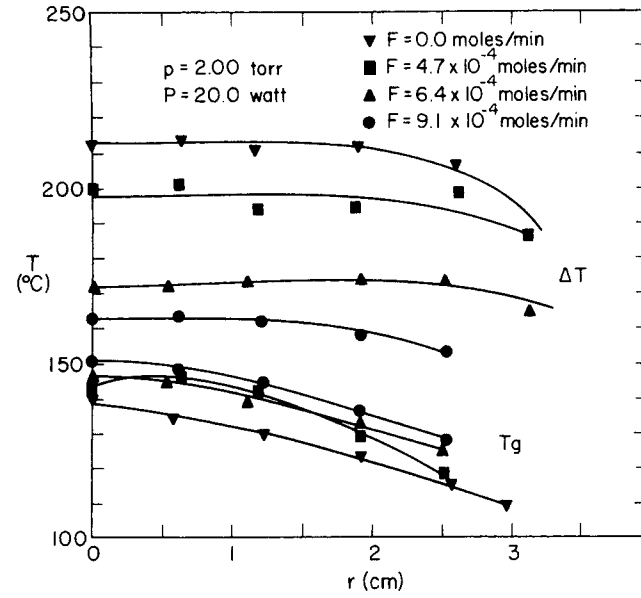

Fig. 8. T_g and ΔT versus flow rate.

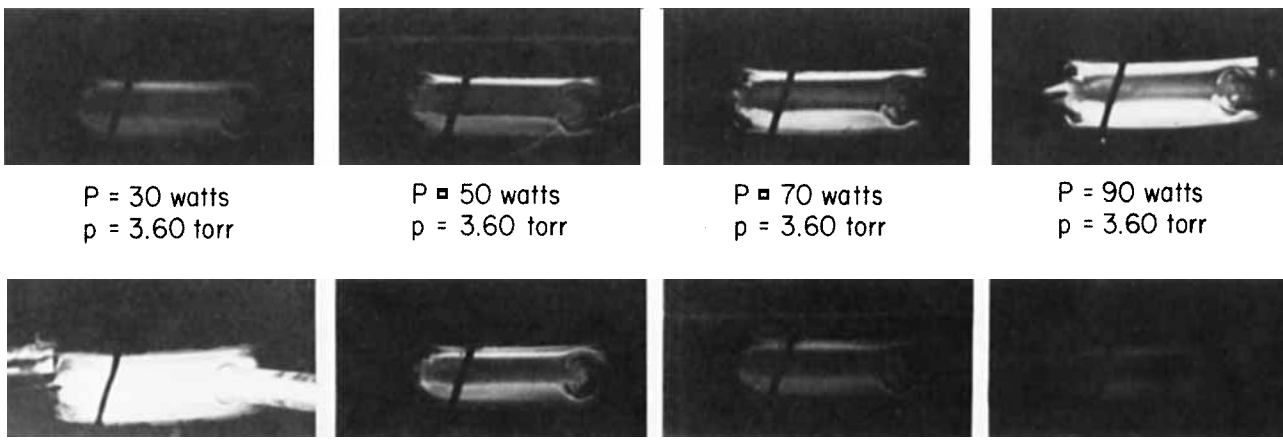

Fig. 9. Photographic observations of the distribution of glow intensity.

10 illustrates k_1 as a function of T_e.

Recombination of atomic oxygen can occur in the gas phase via several paths

$$(2)\quad 2O + O_2 \rightarrow 2O_2$$
$$(3)\quad 3O \rightarrow O + O_2$$
$$(4)\quad O + 2O_2 \rightarrow O_3 + O_2$$
$$(5)\quad O + O_3 \rightarrow 2O_2$$

Rate constants for these reactions at 25°C are listed in Table 1. Atomic oxygen is also lost through heterogeneous recombination on the walls of the reactor. In this instance the effectiveness of the walls in performing the recombination is expressed in terms of the coefficient γ. The value of γ for oxygen recombining on Pyrex is also given in Table 1.

The continuity equation for atomic oxygen can be expressed as

$$\frac{4FN}{(2N - n_1)^2}\frac{dn_1}{dV} = 2k_1\langle n_e\rangle (N - n_1) - \frac{1}{2L} n_1 v_r \gamma - 2k_2 n_1^2 (N - n_1) - 2k_3 n_1^3 - 2k_4 n_1 (N - n_1)^2 \quad (2)$$

where F is the flow rate of molecular oxygen fed to the reactor, V is the reactor volume, L is the spacing between the parallel dielectric walls, and v_r is the random velocity of oxygen atoms. In formulating Equation (2) diffusion perpendicular and parallel to the direction of flow has been neglected. A previous analysis of a similar problem (Bell, 1971) has shown that the diffusion rate is fast enough to eliminate significant concentration gradients in the direction perpendicular to the flow. Furthermore, since the ratio $k_1\langle n_e\rangle D_{12}/(F/NL^2)^2$ is less than one, diffusion in the direction of flow can also be neglected (Petersen, 1965).

In order to perform a numerical integration of Equation (2) it is first necessary to know k_1 and $\langle n_e\rangle$ for a given set of experimental conditions. As was shown in Figure 10, k_1 is a function of the electron temperature T_e. Thus to determine k_1 it is first necessary to predict T_e.

From a simplified theory of glow discharges it can be shown (von Engel, 1965) that the electron temperature is related to E/p, the ratio of the electric field strength to the gas pressure. In the present work Myers' (1969) calculations of the average electron energy as a function of E/p were used together with the relationship $\bullet = \frac{3}{2} kT_e$ to determine T_e versus E/p. The values of E/p required to maintain a discharge can, furthermore, be determined from the product $p\Lambda$, where $\Lambda = L/\pi$ is termed the diffusion length. Sabadil's (1971) experimental measurements of E/p versus $p\Lambda$ were used for this purpose. Figure 11 illustrates Sabadil's results by a smooth curve drawn through the original data.

Once the value of E/p is known for a given value of $p\Lambda$ it is possible to estimate the average electron density $\langle n_e\rangle$. This is accomplished by making use of an expression for the power density

$$\overline{P} = P/V = \langle n_e\rangle e v_d E \quad (3)$$

where P is the total power dissipated and v_d is the electron drift velocity. Equation (3) can be rewritten in the form

$$\frac{\langle n_e\rangle}{\overline{P}\Lambda} = (e v_d\ p\Lambda\ E/p)^{-1} \quad (4)$$

Since v_d is a function of E/p and E/p is in turn a function of $p\Lambda$, the right-hand side of Equation (3) is a function of $p\Lambda$ alone. Values of $\langle n_e\rangle/\overline{P}\Lambda$ were computed from Equation (4) using the results of Hake and Phelps (1967) for v_d versus E/p. The curve of $\langle n_e\rangle/\overline{P}\Lambda$ as a function of $p\Lambda$ is shown in Figure 11. The maximum in the curve is due to the fact that for small values of $p\Lambda$ E/p increases very rapidly thereby causing a decrease in the value of $\langle n_e\rangle$ needed to maintain a fixed value of $\overline{P}$.

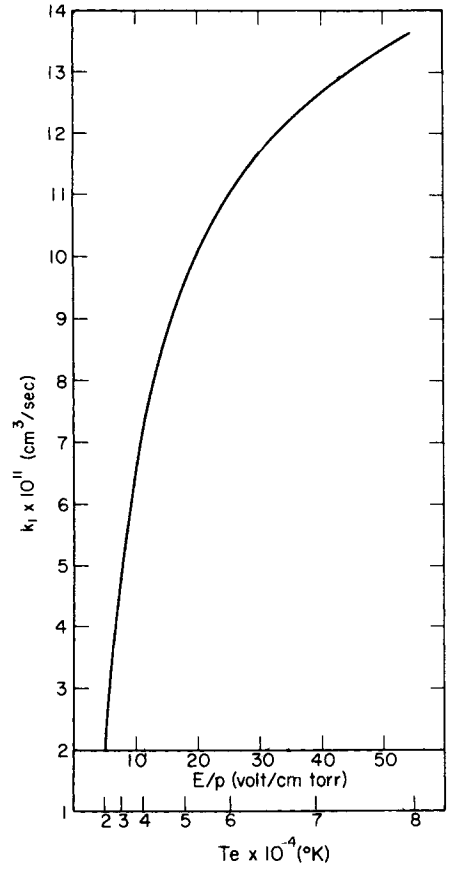

Fig. 10. Dissociation rate constant versus electron temperature and E/p.

TABLE 1. REACTION RATE CONSTANTS AND WALL RECOMBINATION COEFFICIENT

$k_2 = 2.3 \times 10^{-33}$ cm^6/sec	(a)
$k_3 = 1.5 \times 10^{-34}$ cm^6/sec	(a)
$k_4 = 6.4 \times 10^{-34}$ cm^6/sec	(b)
$k_5 = 6.2 \times 10^{-15}$ cm^3/sec	(b)
$\gamma = 1.2 \times 10^{-4}$	(c)

All constants are evaluated at T_g = 298°K. (a) Schofield, 1967; (b) Johnston, 1968; (c) Linnett and Marsden, 1956.

Theoretical Predictions

Based on the development presented above the concentration of atomic oxygen produced by the discharge can be expressed in terms of the variables p, Λ, P, F, and V. Figures 12 and 13 show the predicted conversion as a function of power and pressure in the absence of gas flow. Figure 14 shows the effects of a variation in F/V for a fixed power density.

The increase in the conversion with power shown in Figure 12 is a direct result of a proportional increase in the electron density (see Figure 11). As the power level is raised the slopes of the curves in Figure 12 decrease. This pattern is due to a decrease in the concentration of

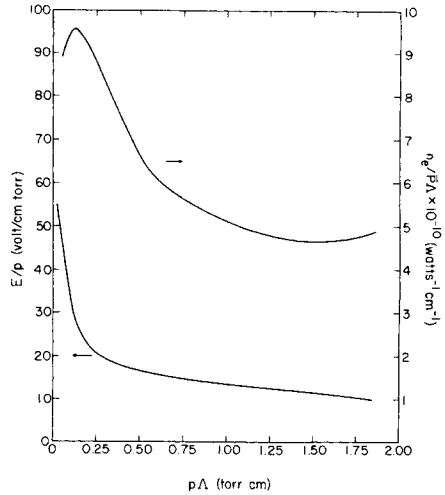

Fig. 11. E/p and $n_e/\bar{P}\Lambda$ versus $p\Lambda$.

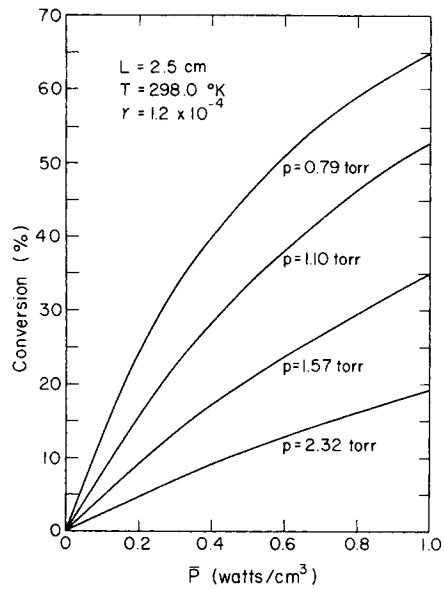

Fig. 12. Theoretical predictions of conversion versus power.

molecular oxygen as the extent of the dissociation is increased which in turn causes a reduction in the rate of dissociation. The increased concentrations of atomic oxygen also lead to an increase in the rates of three-body recombination reactions.

As can be seen from Figure 13 the model predicts a decrease in the steady state conversion as the pressure is increased. This behavior can be ascribed to three factors —a decrease in E/p and hence k_1, a decrease in $\langle n_e \rangle$, and an increase in the rates of the homogeneous recombination processes. At the lowest pressures shown in Figure 13 the curves display a decrease in the negative slope, indicative of an approach to a maximum. Examination of the model shows a maximum should in fact occur at a sufficiently low pressure. The reason for such a maximum can be explained as follows. At very low pressures the value of E/p rises rapidly. This causes k_1 to increase. However, the increase in k_1 is not indefinite and k_1 finally reaches a maximum value as E/p is increased to very large values. Concurrent with the increase in E/p, $\langle n_e \rangle$ falls (see Figure 11) towards zero. The net effect of these trends will be to cause the rate of dissociation to decrease with pressure for sufficiently reduced pressures. Calculations of the conversion could not be extended to low enough pressures to illustrate the complete shape of the maximum due to the absence of data on E/p versus $p\Lambda$ for very small values of $p\Lambda$.

In the presence of a flow of gas the conversion decreases as the value of F/V is increased. This effect which is shown in Figure 14 results from a reduction in the residence time. The yield, on the other hand, is predicted to increase for an increase in F/V.

For small values of F/V the conversion is reduced for an increase in pressure. This trend is reversed, however, at higher values of F/V. An explanation for the inversion can be given in terms of Equation (2). For large values of F/V the loss of atomic oxygen by convection dominates over all other loss processes. As a result Equation (2) reduces to

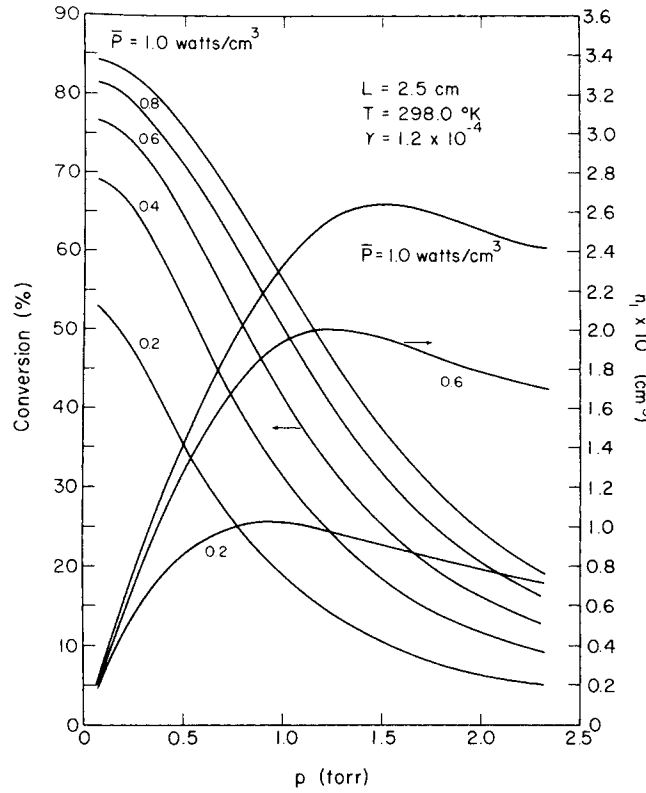

Fig. 13. Theoretical predictions of conversion and atomic oxygen concentration versus pressure.

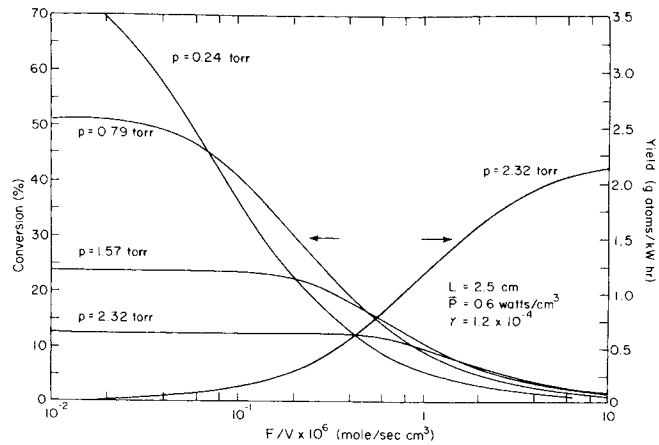

Fig. 14. Theoretical predictions of conversion and yield versus flow rate.

$$\frac{4FN}{(2N - n_1)^2}\frac{dn_1}{dV} = 2k_1\langle n_e\rangle (N - n_1) \qquad (5)$$

Equation (5) can now be replaced by that for a backmix reactor since at low conversions backmix and plug flow reactors give essentially identical results. Thus we may write

$$\frac{2n_1F/V}{(2N - n_1)} = 2k_1\langle n_e\rangle(N - n_1) \qquad (6)$$

From Equation (6) we can see that for a fixed value of F/V the value of n_1/N depends on the product $k_1\langle n_e\rangle N$. Computations of this product using the values of k_1 and $\langle n_e\rangle$ obtained from Figures 10 and 11 show that the product increases with pressure which consequently forces n_1/N to increase with pressure.

Comparison of Theoretical and Experimental Results

A comparison of the calculations shown in Figures 12 to 14 with the experimental data shown in Figures 3a to 5a shows that the reactor model predicts the correct qualitative relationship between the conversion and the experimental variables. The only exception to this is the inversion in the effect of pressure at high F/V shown in Figure 14. This suggests that the variations of k_1 and $\langle n_e\rangle$ with pressure are not accurately portrayed by Figures 10 and 11.

Difficulties are encountered when one wishes to make a quantitative comparison between the predictions and the data. The central problem here concerns the definition of the effective reactor volume. Two reasons can be given for believing that the effective volume does not correspond to the total reactor volume (125 cm^3). First, the geometry of the reactor suggests that gas flow will occur in such a manner that the gas flows through only a fraction of the reactor volume, the balance of the volume containing essentially stagnant gas. The second piece of evidence is the constancy of the yield versus flow rate curves shown in Figure 5b. The fact that the yield is essentially constant is surprising since similar curves obtained for oxygen dissociation by microwave discharges in a tubular reactor (Mearns and Morris, 1971) display an increasing yield with flow rate. The proposed kinetic model also indicates that the yield should increase with flow rate. One is therefore led to believe that the effective volume decreases with increasing flow rate.

In the absence of information regarding the variation of the effective volume with flow rate we cannot obtain an extensive comparison between the model and the experimental data. We can, however, estimate the size of the effective volume by forcing an agreement for a chosen set of experimental conditions. The results of such a fit are shown in Table 2. The calculated effective volume is 11.7 cm^3 or 9.4% of the total value. This figure represents a volume three times that which would be swept out by a disc the diameter of the inlet tube projected across the diameter of the reactor. If the reactor volume is taken as 11.7 cm^3 the corresponding yield would be 1.18 g-atom/kwhr, a figure which is in close agreement with the observations of Mearns and Morris (1971).

Table 2. Conditions Chosen for the Fit of Experiment and Theory

p	= 2.42 torr
F	= 8.4×10^{-4} moles/min
P	= 75 watts
V_e	= 11.7 cm^3

If one accepts the premise that the effective volume should be independent of the power supplied to the discharge, it is possible to compare the predicted variation of conversion versus power with the experimental data. Using the effective volume given in Table 2, the conversion as a function of power was determined by integration of Equation (2). The results appear as the dashed curve in Figure 5a. The experimental and theoretical curves are seen to agree at the point where the fit was forced but diverge otherwise. Furthermore, the slope of the theoretical curve is seen to decrease more slowly with power than that of the experimental curve. A possible explanation for the increasing divergence of the two curves at higher powers could be a neglect in the model of the increase in gas temperature with power. An elevation in the gas temperature can have two effects. One is to reduce the gas density, thereby lowering the dissociation rate. The second is to increase the surface recombination ratio γ. An increase in the value of γ with increasing power would lead to a prediction of smaller conversions than those determined for a constant value of γ.

A final point of comparison can be established by examining the variation in atom concentration with pressure for a fixed power. In Figure 13 the atom concentration predicted by the model is shown for three power densities. Each of the curves is seen to possess a maximum in the range of 2-3 torr. As the power density is increased the maximum shifts to higher pressures. This trend is qualitatively consistent with the probe measurement shown in Figure 7b.

Distribution of Gas Temperature and Atom Concentration

The radial profile of the gas temperature at the midplane of the discharge was shown in Figure 8. From this figure it can be seen that the gas temperature steadily decreases from the center of the discharge to the cylindrical wall. With the exception of the points for 4.7×10^{-4} moles/min the shape of the profile is independent of gas flow rate. A second feature to be noted is the decrease in gas temperature with decreasing gas flow rate. An explanation for this effect can be sought in terms of the composition of the gas in the reactor. At lower flow rates the extent of dissociation is increased, leading to a gas containing more atomic oxygen. Because the thermal conductivity of atomic oxygen is greater than that of molecular oxygen the loss of heat by conduction will be enhanced by the presence of a large fraction of atoms. As a result the gas composition present at low flow rates should cool more rapidly and attain a lower temperature than the gas present at high flow rates.

The distribution of atomic oxygen within the reactor was measured by the temperature difference between a catalytic and a noncatalytic thermocouple inserted into the discharge. These results were presented in Figure 8. Here it can be noticed that for each flow rate the atomic concentration is fairly constant except in the vicinity of the wall (r = 4 cm) where the concentration decreases. The shape of these curves suggests that the diffusion rates of atomic oxygen are sufficiently high to remove significant gradients in concentration. It should be noted that as the flow rate is increased the value of ΔT decreases, indicating a reduction in atom concentration. This behavior is completely consistent with that observed by titration (Figure 5a).

Distribution of Power

The photographs presented in Figure 9 show that the distribution of light intensity within the discharge is not uniform. Since the intensity of the glow can be correlated with power density this suggests that the discharge power

is also distributed nonuniformly. A possible explanation for these observations can be given in terms of the electric field strength distribution in the space between the two electrodes.

It has been shown in a previous study (Bell, 1970) that the local electric field strength in a high frequency discharge sustained between parallel electrodes can be expressed as

$$E = E_0 \left[\frac{(r_0 - 1)^2 + \alpha^2}{(r - 1)^2 + \alpha^2} \right]^{1/2} \tag{7}$$

where $\alpha = \nu/\omega$,

$r = n_e e^2/m_e \epsilon_0 \omega^2$,

and n_e is the local electron density. The subscript zero denotes conditions at the midplane of the discharge. If $r < \alpha$ the electric field has a constant value of E_0. If $r > \alpha$ the electric field has a minimum value of E_0 at the midplane and rises to a maximum value at some point very near to the containing walls. Since the power density is proportional to the product of the electron density and the electric field strength squared, the distribution of power density will reflect the shape of the distribution of electric field strength. Thus for conditions such that $r < \alpha$, the power density distribution will have a shape identical to that of the electron density distribution. Alternatively when $r > \alpha$, the power density distribution will take on a form which has a minimum value at the midplane and reaches a maximum at a short distance from the walls. Consequently if $r > \alpha$ one would expect to see a nonuniform glow which is most intense near the walls to which the electrodes are attached. Estimates of r and α have been made for the present experimental conditions. For a pressure of 2 torr and a power density of 0.6 watts/cm^3 $r = 2.1 \times 10^4$ and $\alpha = 8.2 \times 10^1$. From these values we see that $r > \alpha$ so that the condition required for a nonuniform glow is satisfied.

ACKNOWLEDGMENT

The authors would like to thank the National Science Foundation for the support of this work under Grant GK-4918.

NOTATION

D_{12} = diffusivity of atomic oxygen through molecular oxygen, cm^2/sec
E = electric field strength, V/cm
e = charge on the electron, coul
F = molar flow rate, moles/min
k = Boltzman constant, erg/°K
k_i = reaction rate constant, cm^3/sec or cm^6/sec
L = gap length, cm
m_e = mass of the electron, gm
N = total gas concentration, cm^{-3}
n_1 = atomic oxygen concentration, cm^{-3}
$\langle n_e \rangle$ = volume averaged electron density, cm^{-3}
P = power, watts
$\overline{P}$ = power density, watts/cm^3
p = pressure, torr
r = dimensionless electron density (see Equation 7)
T_e = electron temperature, °K
T_g = gas temperature, °C
ΔT = temperature difference, °C
V = volume, cm^3
V_e = effective volume, cm^3
v_d = drift velocity, cm/sec
v_r = random velocity, cm/sec

Greek Letters

α = dimensionless collision frequency (see Equation 7)
γ = recombination coefficient
ϵ = energy, erg
ϵ_0 = permittivity of space, f/m
Λ = characteristic length, cm
ν = elastic collision frequency, sec^{-1}
ω = source frequency, rad/sec
σ_i = reaction cross section, cm^2

LITERATURE CITED

Bell, A. T., "Spatial Distribution of Electron Density and Electric Field Strength in a High-Frequency Discharge," *Ind. Eng. Chem. Fundamentals Quart.*, **9**, 160 (1970).

———, "A Model for the Dissociation of Hydrogen in an Electric Discharge," *ibid.*, **11**, 209 (1972).

Elias, L., E. A. Ogryzlo, and H. I. Schiff, "The Study of Electrically Discharged O_2 by Means of an Isothermal Calorimetric Detector," *Can. J. Chem.*, **36**, 1680 (1959).

von Engel, A., Ionized Gases, Oxford Univ. Press, New York (1965).

Francis, P. D., "The Production of Oxygen Atoms in a Microwave Discharge and the Recombination Kinetics in a Gas Flow System," *Brit. J. Appl. Phys.*, **22**, 1360 (1954).

Hake, R. D., and A. V. Phelps, "Momentum-Transfer and Inelastic-Collision Cross Sections for Electrons in O_2, CO, and CO_2," *Phys. Rev*, **158**, 70 (1967).

Irving, S., "A Dry Photoresist Removal Method," in *Proc. of Kodak Photoresist Seminar*, Vol. 2, pp. 26-29 (1968).

Johnston, H. S., "Gas Phase Reaction Kinetics of Neutral Oxygen Species," National Standards Reference Data Service, National Bureau of Standards, NSRDS-NBS 20 (1968).

Kaufman, F. K., "Reactions of Oxygen Atoms," in Progress in Reaction Kinetics, Vol. 1, Pergamon Press, New York (1961).

Ligenza, J. R., "Silicon Oxidation in an Oxygen Plasma Excited by Microwaves," *J. Appl. Phys.*, **36**, 2703 (1965).

Linnett, J. W., and D. G. Marsden, "The Kinetics of the Recombination of Oxygen Atoms at a Glass Surface," *Proc. Roy. Soc.*, **A234**, 489 (1956).

McCarthy, R. L., "Chemical Synthesis from Free Radicals Produced in Microwave Fields," *J. Chem. Phys.*, **22**, 1360 (1954).

Mearns, A. M., and A. J. Morris, "Use of the Nitrogen Dioxide Titration Technique for Oxygen Atom Determination at Pressures above 2 Torr," *J. Phys. Chem.*, **74**, 3999 (1970).

———, "Oxidation Reactions in a Microwave Discharge: Factors Affecting Efficiency of Oxygen Atom Production," *Chem. Eng. Progr. Symp. Ser. No. 112*, 37 (1971).

Myers, H. J., "Analysis of Electron Swarm Experiments in Oxygen," *J. Phys.*, **B2**, 393 (1969).

O'Hanlon, J. F., "Plasma Anodization of Metals and Semiconductors," *J. Vac. Sci. Technol.*, **7**, 330 (1970).

Petersen, E. E., Chemical Reaction Analysis, Prentice-Hall, Englewood Cliffs, N. J. (1965).

Sabadil, H., "Zum Mechanismus der Homogen Positiven Säule der Sauerstoff-Niederdruckentladung," *Beitr. Plasmaphys.*, **11**, 53 (1971).

Secrist, D. R., and J. D. Mackenzie, "Vapor Phase Formation of Noncrystalline Films by a Microwave Discharge Technique," *Advan. Chem. Ser., No. 80*, 242 (1969).

Schofield, K., "An Evaluation of Kinetic Rate Data for Reactions of Neutrals of Atmospheric Interest," *Planet. Space Sci.*, **15**, 643 (1967).

Schulz, G. J., and J. T. Dowell, "Excitation of Vibrational and Electronic Levels in O_2 by Electron Impact," *Phys. Rev.*, **128**, 174 (1962).

Manuscript received March 6, 1972; revision received May 4, 1972; paper accepted May 4, 1972.